International Journal of Pharmacy
Journal Homepage: http://www.pharmascholars.com

Original Article **CODEN: IJPNL6**

CO-CRYSTAL CHARACTERIZATION OF NICOTINAMIDE AND UREA

Yutaka Inoue [1,*], Hirotaka Onoda[1], Hiroyasu Sato[2], Isamu Murata[1], Ikuo Kanamoto[1]

[1]Laboratory of Drug Safety Management, Faculty of Pharmaceutical Science, Josai University, 1-1, Keyakidai, Sakado-shi, Saitama 3500295, Japan
[2]Rigaku Corporation, 3-9-12, Matubaratyou, Akishima-shi, Tokyo 1968666, Japan

***Corresponding author e-mail:** yinoue@josai.ac.jp

Received on: 20-06-2016; Revised on: 18-07-2016; Accepted on: 30-08-2016

ABSTRACT

Aim of this study, a co-crystal (nicotinamide and urea) was prepared, and it was used to investigate the relevance of single-crystal structure analysis in combination with other measurement techniques. Results of both single-crystal X-ray diffraction and powder X-ray diffraction confirmed that the nicotinamide and urea co-crystals had a molar ratio of 2/1 and comprised a monoclinic system. Results of differential scanning calorimetry showed that the melting point of the co-crystals was different from that of nicotinamide and urea alone. Results of Fourier transform infrared (FT-IR) absorption spectrometry showed that the co-crystals interacted between nicotinamide and urea due to amino group. Scanning electron microscopy results showed that the co-crystal and nicotinamide and urea alone have different appearances. Thus, the combination of single-crystal structure analysis with other measurement methods is very useful for analyzing the crystal structure in detail.

Keywords: Co-crystal, Nicotinamide, Urea, Single crystal, Characterization, FT-IR

INTRODUCTION

Improvement of solubility, bioavailability, and stability of pharmaceutical products is an important issue. Solubility can be enhanced by using cyclodextrins or by salt formation, such as a sulfate or hydrochloride salts [1,2]. Recently, co-crystal technology is being rapidly developed for use in drug discovery and development of pharmaceutical products [3]. There are various definitions of a "co-crystal;" according to one source, co-crystals are "stoichiometric multicomponent crystals in which all of the components are, when pure, solids under ambient conditions." [4] Generally, co-crystals are made by a slurry method, an evaporation method, or a vapor phase–liquid phase diffusion method. These techniques for the preparation of co-crystals are used to create pharmaceuticals. For example, niacin present in the vitamin B group, the use of co-crystals of alias nicotinamide, carbamazepine, ibuprofen, theophylline, and the like have been reported [5–7]. In addition, urea has been used as a co-crystal material; for example, in the urea/indomethacin co-crystal (indomethacin is an anti-inflammatory agent) [4]. Nicotinamide and urea are used to enhance the solubility of poorly soluble pharmaceuticals as these materials are water-soluble and have low human toxicity. Characterization of co-crystals is typically performed by single-crystal structure analysis using X-ray diffraction. However, only a few cases have been reported on combined methods, such as FT-IR and PXRD. The purpose of this study was to characterize co-crystal of nicotinamide and urea by single-crystal structure analysis. PXRD, FT-IR, DSC, and SEM evaluated the physico-chemical properties of the co-crystal in the powder state.

MATERIALS AND METHODS

Reagents: Nicotinamide (NA) and urea (UR) were purchased from Wako Pure Chemical Industries, Ltd.

(Japan). The purity was 98%. Other reagents were also obtained from Wako Pure Chemical Industries.

Sample preparation: A physical mixture (PM) of NA and UR (total mass = 0.1 g; molar ratio = 1/1) was prepared by stirring for 1 min with a vortex mixer. The evaporated amount (EVA) is mixed with NA and UR in a molar ratio of 2/1, 1/1, and 1/2 (total mass = 0.1 g). The resulting mixture was dissolved in methanol (20 mL), and purified by solvent distillation at 40°C and 25 rpm.

NU co-crystals were prepared by mixing NA and UR in a molar ratio of 1/1 (total amount = 0.5 g), and they were then dissolved in methanol (3.5 mL) in a test tube. Then, the test tube was placed in a co-stoppered Erlenmeyer flask using toluene as a poor solvent, and was allowed to stand at room temperature with the plug. The grown crystals were washed with toluene and stored in toluene until the measurement. Next, 0.5 g of NA was weighed and dissolved in methanol (3.5 mL). The test tube was placed in an Erlenmeyer flask with toluene as a poor solvent, and allowed to stand at room temperature with the plug. UR was prepared in the same way. All resulting crystals were washed with toluene and stored in it until the measurement.

Single-crystal X-ray diffraction (SXRD): The SXRD was measured using an IP Weissenberg automatic X-ray analyzer (R-AXIS RAPID-S, Rigaku) under a nitrogen atmosphere at -100°C using Mo K_α line (λ = 0.71075 Å, 50 kV, 30 mA) as the X-ray source. The analysis was carried out using SIR92 (direct method), and the refinement was conducted using SHELXL-2014. The density (g/cm^3) was computed as follows:

$$ {}^{g}/_{cm^3}\,(\text{Density}) = \frac{(1 \times 10^7)^3}{V \times 6.02 \times 10^{23}} \times MW \times N $$

V: cell volume ($Å^3$)
MW: one-unit molecular weight (g/mol)
N: number of unit cells

Coordinates have been deposited at the Cambridge Structure DataBank (CCDC codes 1445331) and are available as supplementary material to this article.

X-ray powder diffraction (PXRD): The Mini FlexII PXRD device (Rigaku) was used. Cu Kα radiation (λ = 1.54184 Å, 30 kV, 15 mA) through a Ni filter was used as the X-ray source. The diffraction strength was measured by a NaI scintillation counter. The following Measurement conditions were used: scan speed, 4°/min; scan measurement range, 2θ = 5°–35°.

Differential scanning calorimetry (DSC): DSC measurement was carried out by putting 2 mg of the sample in an aluminum hermetic pan. A Thermo plus Evo high-sensitivity differential scanning calorimeter (Rigaku) was used under a nitrogen gas flow (60 mL/min) and the temperature was increased at a rate of 5°C/min.

Infrared (FT-IR) absorption spectroscopy: The sample was prepared by the KBr tablet method. FT-IR spectroscopy was measured using JASCO FT/IR-460Plus (manufactured by JASCO oration) under the following conditions: accumulated number of times = 16, resolution = 1 cm^{-1}, and measurement range = 4000–400 cm^{-1}.

Scanning electron microscopy (SEM): For SEM measurements (S3000N Scanning Electron Microscope, Hitachi High-Technologies Corporation), samples were subjected to 70 s of gold deposition under an acceleration voltage of 10 kV.

RESULTS AND DISSCUTION

Study of Single-crystal X-ray diffraction: The crystal structure of NU was analyzed by SXRD measurements (Fig. 1 (c)). The crystal structures of NA and UR alone were also measured to compare them with the crystal structure of NU (Fig. 1 (a), (b)). NA and UR single crystals had the monoclinic and tetragonal systems, respectively [8, 9]. Based on the ORTEP diagram shown in Fig. 1, the following is confirmed: molar ratio of NA/UR = 2/1, and space group = P 21/n (monoclinic system) (Table 1). UR formed a sheet-like structure by forming hydrogen bonds (Fig. 2). NA forms hydrogen bonds with the carbonyl group and the amide groups of UR, denoted as $R_2^2(8)$ in graph set notation, and these bonds were found to repeat.

Table 1. NU Crystal data

parameter	NU
formula	$C_{13}H_{16}N_6O_3$
stoichiometry	2/1
formula weight	304.31
crystal system	monoclinic
space group	$P\ 2_1/n1$
a (Å)	7.2537(13)
b (Å)	11.535(2)
c (Å)	17.136(3)
α (deg)	90.000
β (deg)	91.102(6)
γ (deg)	90.000
volume ($Å^3$)	1433.4(5)
calc density ($g\ cm^{-3}$)	1.41
Z	4
T (K)	173(2)
R1	0.0655
wR2	0.1601

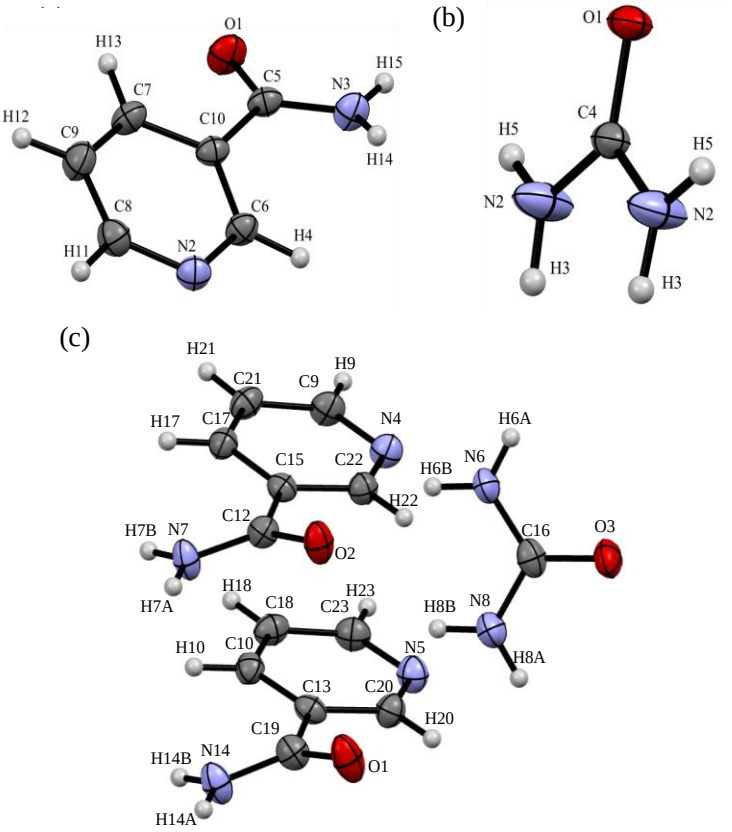

Fig. 1. ORTEP Figure (a) NA, (b) UR, (c) NU, Displacement ellipsoids are drawn at the 50% level.

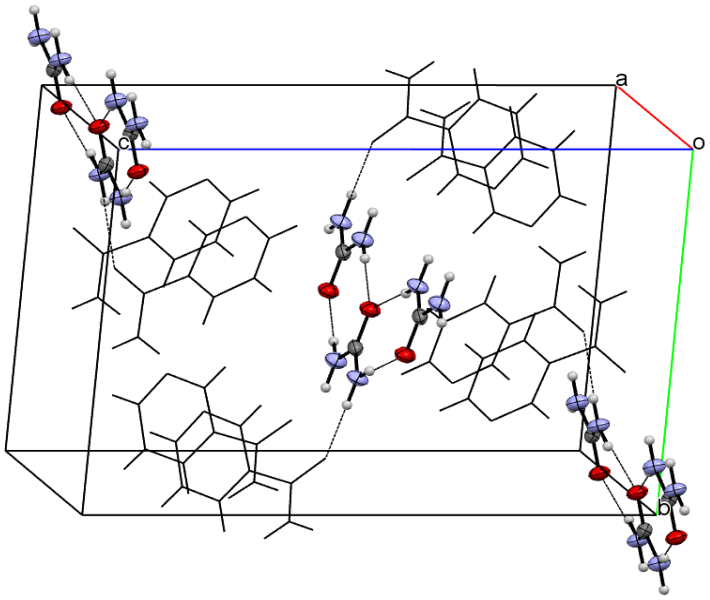

Fig. 2. NU Crystal is UR band

PXRD: PXRD measurement were carried out to evaluate the crystal state of each sample and determine the validity of the single-crystal structure analysis results. The characteristic peaks of NA were observed at 14.6°, 23.3°, and 27.3°, and that of UR was observed at 29.3° (Fig. 3 (a), (b)). The peaks of NA and UR alone in PM were also identified (Fig. 3 (c)). EVA 2/1 produced characteristic peaks at 9.0°, 10.1°, and 16.2° (Fig. 3(d)). EVA1/1 also produced characteristic peaks at 9.0°, 10.1°, and 16.2° (Fig. 3(e)). EVA1/2 produced a characteristic peak at 16.2° (Fig. 3(f)). In addition, EVA2/1 produced a pattern that matched the PXRD pattern that was predicted on the basis of its SXRD pattern (Fig. 3(d), (g)). These findings indicate that EVA2/1 and NU have the same crystal structure.

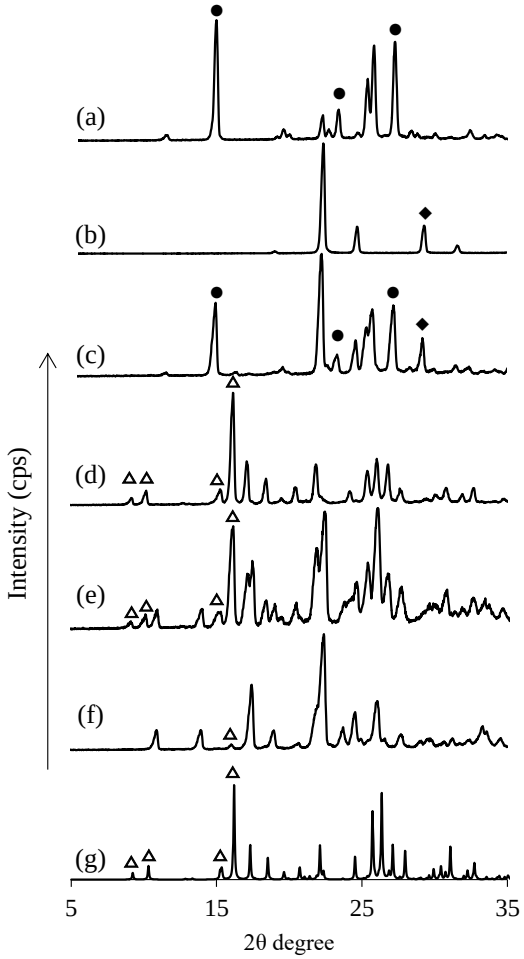

Fig. 3. PXRD patterns of (a) NA, (b) UR,
(c) PM(NA/UR=1/1), (d) EVA(NA/UR=2/1),
(e) EVA(NA/UR=1/1), (f) EVA(NA=1/2),
(g) NU PXRD sim.
●:Specific peak of NA, ◆:Specific peak of UR,
△:Specific peak of NU

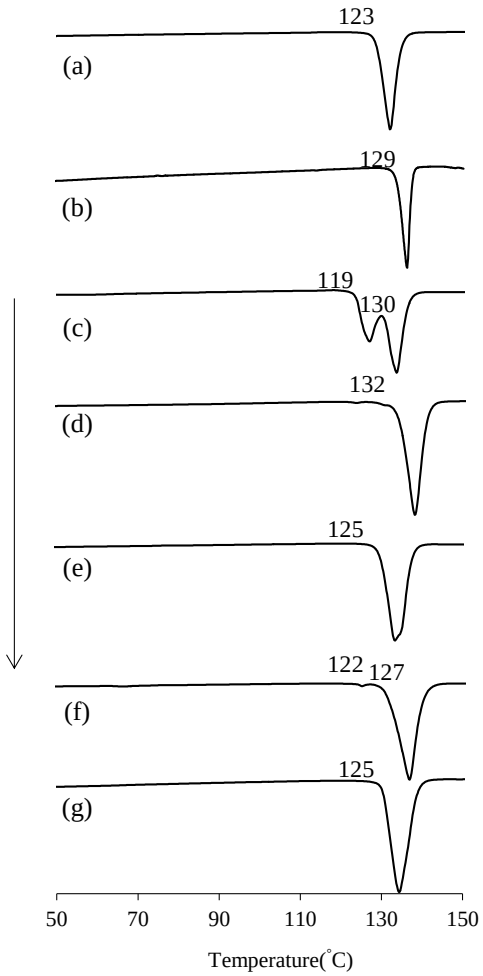

Fig. 4. DSC curves of (a) NA, (b) UR,
(c) PM(NA/UR=1/1), (d) EVA(NA/UR=2/1),
(e) EVA(NA/UR=1/1), (f) EVA(NA/UR=1/2),
(g) NU

Evaluation of DSC: DSC measurements were carried out to determine the change in the melting point of each crystal. The NA and UR melting points were 123°C and 129°C, respectively, while their melting points in the PM are 119°C and 130°C, respectively (Fig. 4 (a), (b), (c)). The endothermic peak for EVA2/1 was observed at 132°C; that for EVA1/1 was observed at 125°C; and those of EVA1/2 were observed at 122°C and 127°C (Fig. 4 (d), (e), (f)). The melting point of NU was observed at 125°C (Fig. 4 (g)). EVA1/1 produced an endothermic peak that broadened at 125°C,

presumably indicating the existence of 2 melting points. The endothermic peak of EVA1/1 was broad and observed at 125°C, which could be the average of the melting points of its components. The EVA2/1 peak was sharp at 132°C. The above observations suggest that EVA2/1 can exist as a co-crystal or alone. Both EVA1/1 and EVA1/2 are types of co-crystal systems, and NA or UR alone has been estimated to be present in the co-crystal system. PXRD and DSC results indicated that the results of SXRD analysis were valid. In addition, the optimal molar ratio for co-crystals of NA and UR was found to be NA/UR = 2/1.

FT-IR absorption spectrum: FT-IR measurements were carried out to evaluate the molecular interaction in each sample (Fig. 5). The FT-IR absorption spectrum of the NA and UR is already known (Fig. 5 (a), (b)) [10, 11]. The nicotinamide alone was observed, stretching vibration to 3367 cm^{-1} of the N-H, stretching vibration to 1699 cm^{-1} of the C=O, stretching vibration of the 1480 cm^{-1} of the C=C, stretching vibration to 1202 cm^{-1} of the C-NH_2, in-plane bending to 625 and 603 cm^{-1} of the CCC. The urea alone was observed, stretching vibration to 3442 and 3346 cm^{-1} of the N-H, stretching vibration to 1684 cm^{-1} of the C=O. The PM produced peaks at 3438 and 3361 cm^{-1} due to the amide groups of NA and UR, a peak at 1713 cm^{-1} due to the carbonyl group of UR, and peaks at 609 and 592 cm^{-1} due to the pyridine ring of NA (Fig. 5(c)). Compared to NA and UR alone, the PM had a shift in peaks due to the amide groups and the carbonyl group of NA and UR and the pyridine ring of NA, so complexes were formed in the PM. This presumably means that interaction occurred during spectroscopy as a result of the pressure applied to the sample during tableting. In NU, 3475, 3437, and 3344 cm^{-1} peaks were observed owing to the amino group in NA and UR; a peak at 1715 cm^{-1} due to the carbonyl groups of UR and NA and the pyridine ring of NA; and 608 and 594 cm^{-1} peaks were observed owing to the pyridine ring in the NA (Fig. 5 (d)). The results of the crystal structure analysis of the NU show that hydrogen bonds form between the amide group of one NA moiety and the amide group of another NA moiety (Fig. 6).

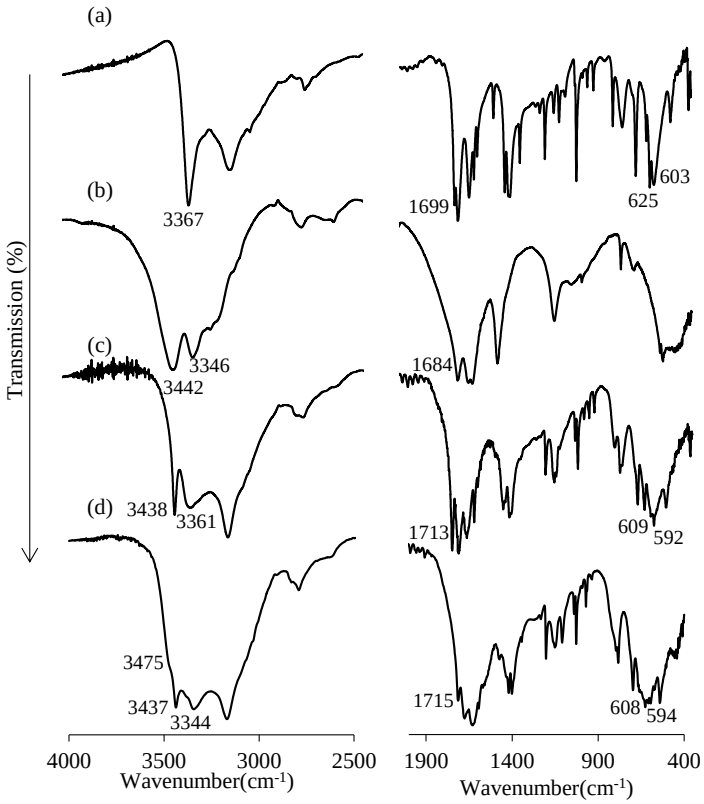

Fig. 5. FT-IR spectra of (a) NA, (b) UR, (c) PM(NA/UR=1/1), (d) NU

The bond distance of the ketone group derived from the NA (1.247 Å) and NU co-crystal is longer than that of the NA alone (1.236 Å), and the bond distance of C-NH_2 is shorter (1.325 Å) in the former than that in the latter (1.334 Å) (Fig. 7 (a), (c)). In addition, in NA, the hydrogen bond distance between the amino group and the ketone group of UR alone is shorter than that in the co-crystal of NU, NA, and UR (Fig. 7). Therefore, the amino group of the NA and UR showed a strong electron-withdrawing effect on the ketone group, whereby an oxygen atom of the ketone group is pulled toward the amino group side and π-electron of the amide group is pulled toward the ketone group side; however, the bond length does not become longer. Hence, the amino group of the NA and the co-crystal of UR and NU form hydrogen bonds with the ketone group, leading to the inductive effect (I effect); this phenomenon gave rise to the high wave shifts in the FT-IR spectra [12].

In the amino group of the NU, compared with the NA and UR alone, the low-frequency side and the shift to high-wave-number side have been confirmed (Fig. 5 (a), (b), (d)). Compared to NA and UR alone, NU had more sites involved in the hydrogen bonding of NA and UR, and this is why absorption shifted to a lower frequency (Fig. 8). Compared to UR alone, NU had bonds that were longer than the C-NH_2 bonds in UR, and this is why absorption shifted to a higher frequency (Fig. 7(b), (d)). It was confirmed that in UR, atoms are on the same plane. However, in the NU, the UR does not occur on the same plane (Fig. 7 (b), (d)). The amino group of UR in the NU weakens the π-bonding, and hence, it was inferred that the single bond becomes stronger. In addition, all the protons derived from the amino group of the NA and UR take part in hydrogen bonding. However, one proton of the UR occurring in NU is not involved in hydrogen bonding (Fig. 8). Thus, free protons may explain the presence of a new peak (Fig. 5).

NU and NA alone were compared, and results indicated that the peak due to the pyridine ring shifted, so molecular interaction between NA and UR occurred. The pyridine ring of the peak shift of NU implies π-π stacking. However, in the NA alone, π-π stacking was not observed. In NU, NA shows π-π stacking between pyridine to form a dimer (Fig. 10). Note that π-π stacking is mainly classified into two configurations: face-to-face and edge-to-face. The face-to-face configuration is further classified into parallel face-centered and parallel offset. In toluene, the edge-to-face configuration is classified into perpendicular t-shaped and perpendicular y-shaped configurations (Fig. 9) [13]. Generally, face-to-face (surface distance = 3.3–3.7 Å) and edge-to-face (face-centered distance = 5.4–7.8 Å) configurations have been reported to occur at a distance [14, 15]. In this experiment, parallel offset and perpendicular y-shaped configurations were confirmed to have bond distances of 3.311 Å and 5.885 Å, respectively.

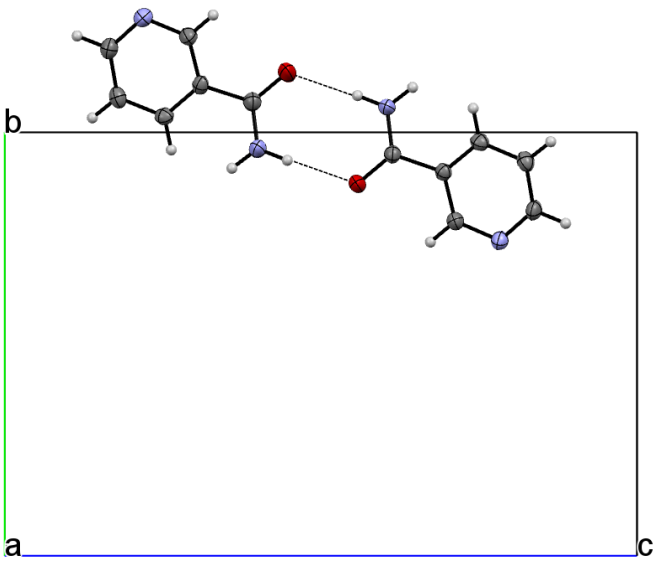

Fig. 6. NA and NA H-bond angle a
Displacement ellipsoids are drawn at the 50% level.
Broken lines is distance of H-bond between the nitrogen and oxygen.

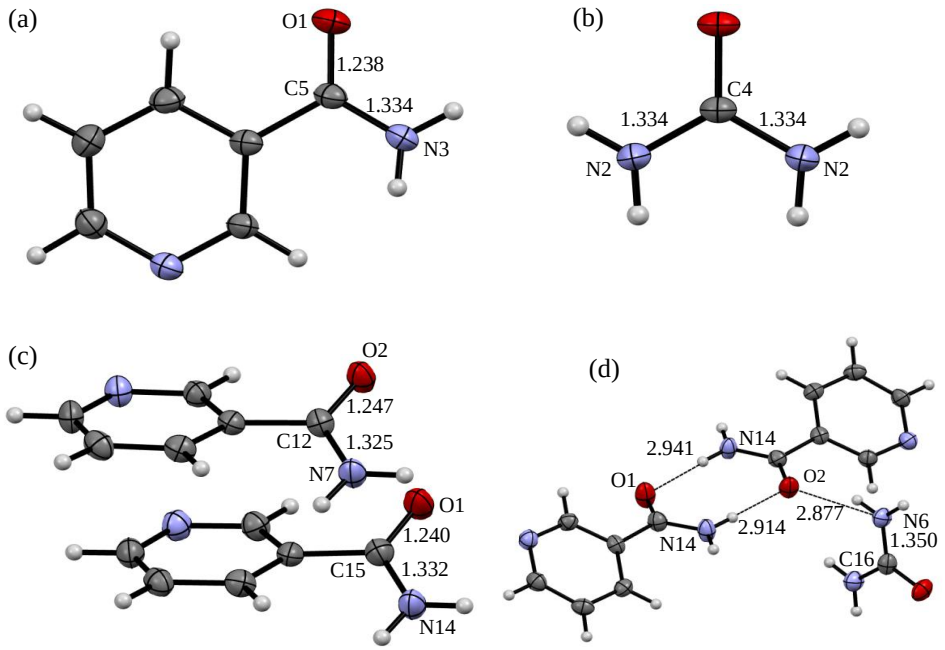

Fig. 7. NA and UR, NU Hbond distance and Bond distance (a) NA, (b) UR, (c) NU, (d) NU Displacement ellipsoids are drawn at the 50% level. Broken lines is distance (Å)

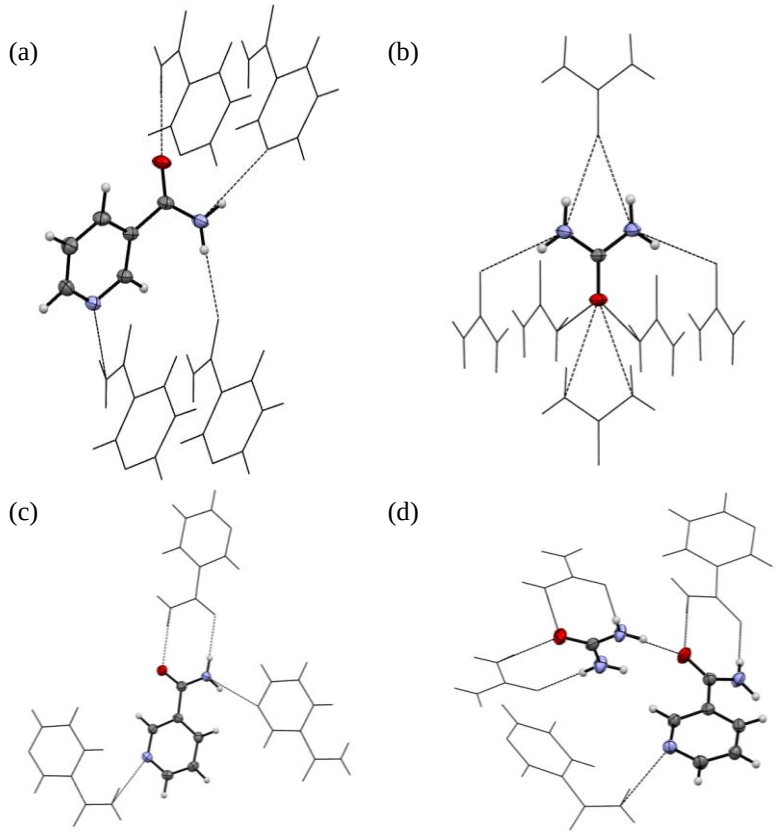

Fig. 8. H-bond of (a) NA H-bond, (b) UR H-bond, (c) NU H-bond 1, (d) NU H-bond 2, Broken lines is H-bond.

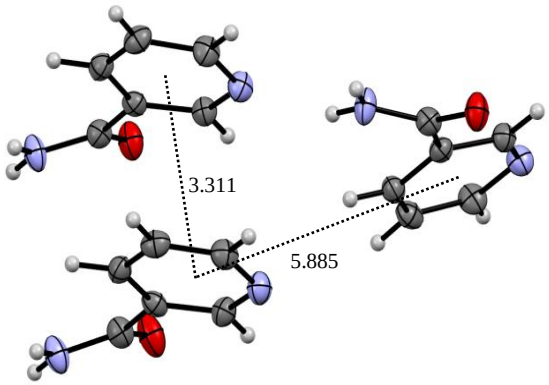

Fig. 9. NA and NA π-π stacking
Displacement ellipsoids are drawn at the 50% level.
Broken lines is distance(Å) of π-π stacking.

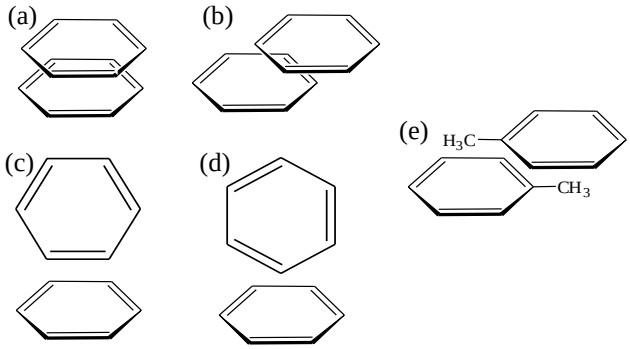

Fig. 10. π-π stacking type of (a) Parallel face-centred,
(b) Parallel offset, (c) Perpendicular t-shaped,
(d) Perpendicular y-shaped, (e) Parallel offset toluene

Morphology by SEM: The crystalline appearance state of each sample was confirmed using SEM (Fig. 10). NA and needle-like crystals in NU were observed. UR was observed to have cube-type crystals. Needle-shaped and cube-shaped crystals were not noted in the PM and EVA. NA and UR have different crystalline states; complex formation was also confirmed. NA and NU have a monoclinic system, while UR occurs in a tetragonal system (a crystal system with a right angle). The crystal systems of NA and NU could not be determined, but UR crystals were found to have axes at right angles. The crystalline appearance of a sample is presumably correlated with its crystal system.

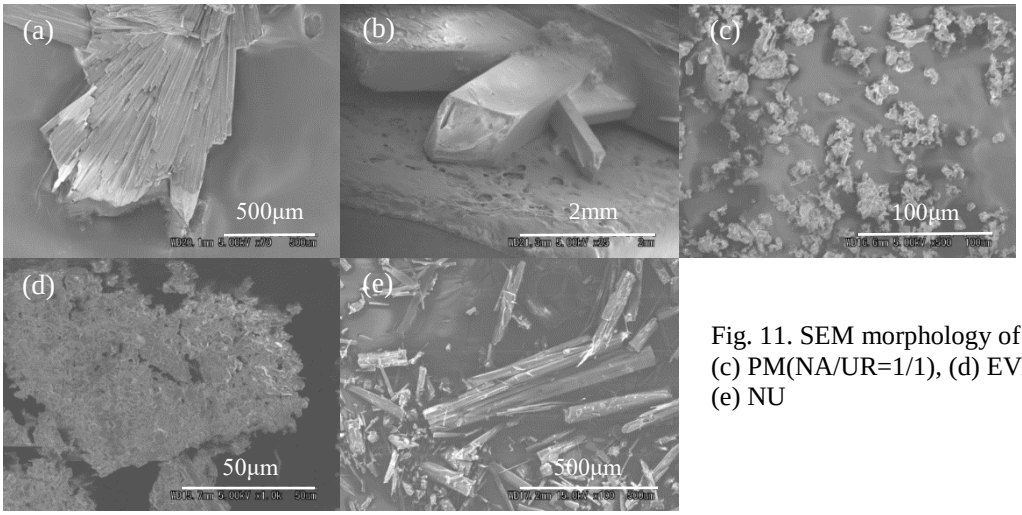

Fig. 11. SEM morphology of (a) NA, (b) UR,
(c) PM(NA/UR=1/1), (d) EVA(NA/UR=1/1),
(e) NU

CONCLUSION

Based on the discussion so far, it can be concluded that NA and UR form a co-crystal in a molar ratio of 2/1. Few previous studies have used techniques such as XRD and IR absorption spectrometry to examine co-crystals. Obtaining a single crystal of some co-crystals is difficult, and the physical properties of those co-crystals need to be assessed with data such as SXRD patterns and IR spectra. Such research will provide valuable information when co-crystals and crystals are structurally analyzed in the future. Further research should be conducted, and research needs to examine the relationship between co-crystals and poorly soluble pharmaceuticals using 2 types of solubilizing agents.

Acknowledgements: We thank Rigaku Corporation and thank Dr. Hiroshi Miyamae at Josai University, Japan, for guidance on single-crystal structural analysis.

Conflict of interest: There is no conflict of interest to report.

REFERENCES

1. Suzuki R, Inoue Y, Tsunoda Y, Murata I, Isshiki Y, Kondo S, Kanamoto I. J Incl Phenom Macro, 2015; 83(1): 177-86.
2. Abu T M S. Adv Drug Deliv Rev, 2007; 59(1): 603-16.
3. László F, Noel H, Kevin S E, Humphrey A M, Anita R M, Linda M C, Simon E L. Cryst Growth Des, 2011; 11(8): 3522-8.
4. Ahmed A M G, Sundos Q. Al-E, Zakia M M, Nihal A, Sara Al-A. American J Adv. Drug Deliv, 2016: 4(1).
5. Shashank P P, Sameer R M, Arvind K B. Eur. J Pharm Sci, 2014; 62(1): 251-7.
6. Jie L, Sohrab R. Org Process Res Dev, 2009; 13(6): 1269-75.
7. David J B, Colin C S, William C, Ross W H, Simon J C, Peter N H, Michael B H, Richard S, William J, Tomislav F, Nicholas B. Cryst Growth Des, 2008; 8(5): 1697-712.
8. Miwa Y, Mizuno T, Tsuchida K, Taga T, Iwata Y. Acta Cryst, 1999; B55: 78-84.
9. Birkedal H, Madsen D, Mathiesen H R, Knudsen K, Weber H-P,. Pattison P, Schwarzenbach D. Acta Cryst, 2004; A60: 371-81.
10. Ramalingama S, Periandyb S, Govindarajanc M, Mohan S. Spectrochim Acta A, 2010; 75(5): 1552-8.
11. Yamaguchi A, Miyazawa T, Shimanouchi T, Mizushima S. Spectrochim. Acta, 1957; 10(2): 170-8.
12. Scarano D, Bertarione S, Spoto G, Zecchina A, Arean O C. Thin Solid Films, 2001; 400(1-2): 50-5.
13. Chelsea R Martinez, Brent L I. Chem Sci, 2012; 3: 2191-201.
14. Christoph J. J Chem Soc Dalton Trans, 2000; 3885-96.
15. Per L. A Am Chem Soc, 1992; 114(11): 4366-73.